Synthesis, characterization and Li adsorption study of a new thermoresponsive crown-ether bearing copolymer

Ariella Liberati, Amine Geneste, Benedicte Prelot, J.P. Mericq, Catherine Faur, Sophie Monge

Synthesis, characterization and Li adsorption study of a new thermoresponsive crown-ether bearing copolymer

Ariella Liberati[a,b], Amine Geneste[a], Benedicte Prelot[a], Jean-Pierre Mericq[b], Catherine Faur[b,*], Sophie Monge[a,*]

[a] ICGM, Univ Montpellier, CNRS, ENSCM, Montpellier, France

[b] IEM, Univ Montpellier, CNRS, ENSCM, Montpellier, France

* Corresponding authors.

E-mail addresses:

catherine.faur@umontpellier.fr (C. Faur), sophie.monge-darcos@umontpellier.fr (S. Monge)

Abstract

With the ever-growing sales of electric vehicles (EVs) in the world and uncontrolled consumption of non-renewable lithium resources for lithium-ion batteries (LIBs), new materials were proposed to reinforce the recycling technologies that are currently in use. For such purpose, the design and synthesis of a new crown ether-bearing monomer, namely 2-(benzo-12-crown-4-ether)ethyl methacrylamide (BCEEM), its copolymerization with N-isopropylacrylamide (NiPAAm) and its adsorption properties were studied. While crown ethers (CEs) are well known for their metal adsorption properties, NiPAAm brought thermoresponsive properties to the copolymer, allowing for sorption at certain temperatures, and great processability through precipitation at other temperatures. With varied BCEEM/NiPAAm ratios, Lower Critical Solution Temperatures (LCST) ranged from 6 to 26.5 °C. Regarding the sorption performances by the CEs, several parameters were varied, such as pH, temperature and Li/CE ratio. Under optimized experimental conditions, the lithium sorption isotherm highlighted a maximum adsorption capacity of 0.075 mmol/g polymer (0.55 mg.g^{-1}), which is in the lower limit compared to similar CE studies reported in the literature. Moreover, competitive sorption studied in multicomponent solutions (Li, Co, Ni, Mn) simulating lithium-ion batteries (LIB) leachates (containing mostly lithium and cobalt), as well as in solutions with increased amounts of nickel and manganese, showed that selectivity towards lithium (and to a lesser extent cobalt) appeared to depend on the relative concentration of these two elements compared to Ni and Mn. In leachate-like conditions, the copolymer showed selectivity towards Li and Co whereas the selectivity evolved towards Ni and Mn as the initial concentration of Ni and Mn increased. DLS and ITC measurements were undergone to comprehend the obtained sorption capacities and selectivity from a mechanistic and thermodynamic point of view. While DLS measurements indicated potential salting-out effect of the ions causing degradation of water and metal interactions with the CEs, ITC experiments shed light on the potential culprit: the rigidity and hydrophobicity of the benzo-group.

Keywords

Graphical abstract
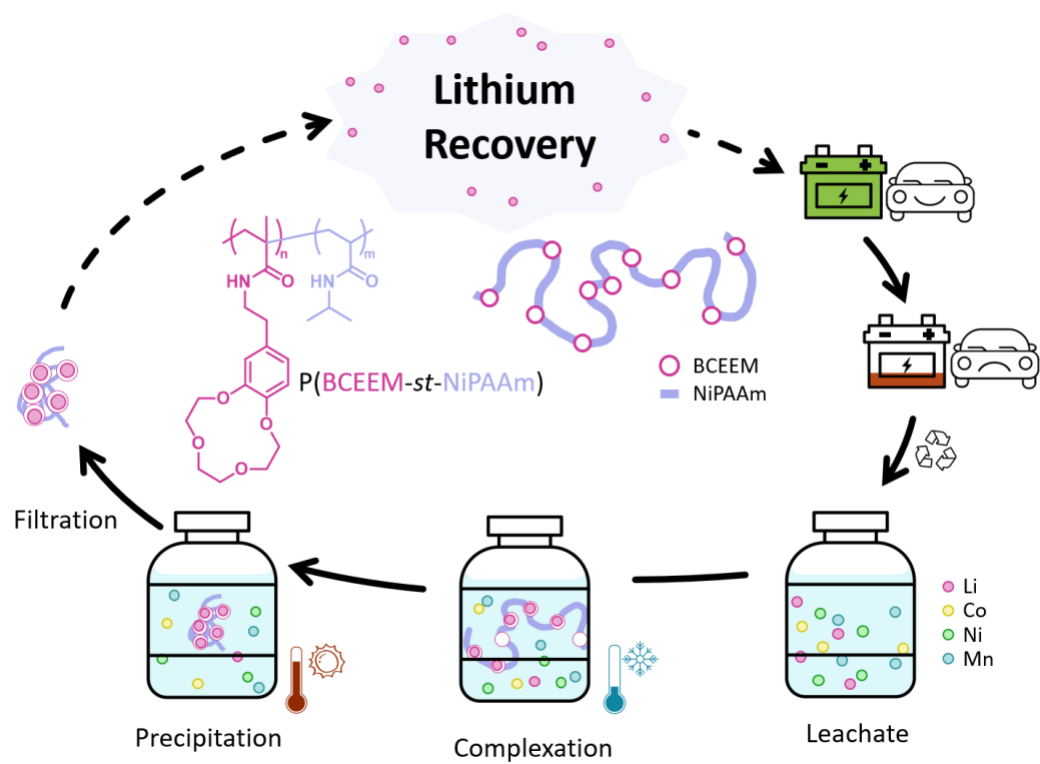
1. Introduction

The development of the electric vehicle (EV) industry over the past decade and the forecasted 23 million EVs sold globally by 2028 has led to a drastic over-consumption of non-renewable resources such as lithium and cobalt [1]. The first marketed EVs were designed with a lifespan ranging from 1 to 10 years [2], depending on the frequency of use, currently generating a significant influx of waste on a global scale. Parallelly, lithium and cobalt are natural non-renewable resources found in mineral ores (or brines for lithium). Their consumption over the past decade has evolved from ceramics, glass and lubricants for lithium and pigments, alloy materials and catalysts for cobalt, towards mostly batteries. For instance, lithium alone has a forecasted consumption of 1.25 million tons in 2028 [3], corresponding to approximately 5% of our global resources for one single year [4]. Accordingly, the European Commission has been imposing stricter regulations on industrials for the collection, separation and reuse of their products to avoid not only the waste of such promising constituents (Li, Co, Ni, Mn, Fe, Cu, etc.), but also the risk of draining our natural resources [5]. Current industrial battery recycling processes, mainly pyrometallurgy and hydrometallurgy, consist in respectively very high temperature calcinations and step-by-step acidic leaching for the selective precipitation of metals. They are employed after discharge, dismantling and pre-treatments steps (mechanical, solvent or low temperature calcinations), on a powder called "active material" consisting of mainly lithium, cobalt, nickel and manganese and allow the separate recovery of each metal at various purities levels usually varying from 96.5 to 99.97 % [6]. Nevertheless, recycling experts are currently struggling with the actual collection step of end-of-life LIBs, creating a gap between our global recycling capabilities, and what is actually recycled currently. Additionally, pyrometallurgy and hydrometallurgy are known for their rather polluting, energy-consuming and onerous drawbacks [7-9]. Metal-selective inorganic materials are described in the literature but remain rather limited to laboratory-scale studies for the moment [10]. For instance, the adsorption processes for the recovery of lithium are mainly described with Mn or Ti-based materials, as ion exchange sieves, providing high capacity, selectivity and good recycling properties. Yet their poor versatility, low reuse frequency, dissolution loss and synthesis (high temperature and energy consuming) have not been fully improved to be implemented in the recycling industry [11].

Organic molecules that are capable of selectively and efficiently interacting and bonding with metal ions have been reported in the literature [12-17]. Notably, crown-ethers (CEs), and more precisely 12-Crown-4 (12C4), are presented in the literature as being selective for Li^+ over plenty of other alkali metal ions. With their ether-containing cyclic configuration, CEs provide host-guest complexation, where the size of their

cavities defines their cation selectivity, and the electron donating oxygen atoms can interact with the positively charged ions [18]. The range of CE efficiencies is rather heterogeneous in the literature, with lithium sorption capacities varying from 14.6 µg.g^{-1} to 27 mg.g^{-1} [14, 19]. Although lithium selectivity is greatly described in the literature, its behaviour has rarely been studied in aqueous solutions originating from LIB recycling, as studies mostly regard synthetic or natural brine solutions containing Na, K, Mg or Ca. In particular, Nisola et al. report the use of dibenzo-14-crown-4-ethers to effectively recover lithium from leachate-like solutions (mainly containing Li, with traces of Al, Co and Cu) with a sorption capacity of 1.373 mmol/g polymer [14]. Li et al, used 12C4-based membranes in batch experiments to efficiently recover lithium from solutions containing Co, Ni and Mn in a 1.5-fold higher concentration than lithium [20]. With a more mechanistic point of view, Sun et al. studied equimolar solutions of Co and Li and observed that liquid-liquid extractions using benzo-15-crown-5-ethers allowed selectivity towards lithium over cobalt with 37 % extraction of lithium against only 5 % for cobalt [21]. With initial Li/M concentrations drastically varying (above or under 1), all three of these studies provide insight into the selectivity of CEs towards lithium over other LIB metals. However, given the scarcity of the studies on leachate-like solutions, and the varying compositions of the solutions used in the existing research, a thorough inventory of leachate solutions described in the literature would be of great interest. From this, a typical average leachate solution could be identified, and a novel study of CE behaviour in this typical solution could be conducted.

12C4 ethers require mild-condition synthesis and offer easy processing and great adaptability. They are reported in various Li$^+$ recycling processes in the form of liquid-liquid extractions (conventional, or in association with ionic liquids) [21-23], adsorption onto macro, micro, or nano particles [24-27] and membranes for dead-end or crossflow processes [28-30], but rarely in single phase separation. In this latter case, the polymers are in fact initially water-soluble, thus enabling faster and better access to the sorbing CE groups since they are in the same phase as the ion, and consequently improves sorption kinetics and capacities. Yet very few lithium-selective water-soluble materials have been described in the literature. Grafting the CE onto a polymeric material enables better processability as the high molecular weight macromolecular structure may be easier to separate from the solution, by filtration for instance. Nevertheless, the solubility of the polymer can be problematic for its post-sorption separation from the effluent, unless potentially energy-intensive membrane techniques are used. An alternative is to use stimuli-sensitive polymers. Indeed, after the sorption step, the polymer can be precipitated by an external stimulus and separated from the solution [31, 32]. Thermoresponsive polymers are great candidates for such processes as their Lower Critical Solution Temperature (LCST) enable them to become insoluble in water when temperature is increased [33]. For instance, Graillot et al. have reported the synthesis of an

original copolymer containing both nickel-selective monomers and an acrylamide that provided thermoresponsive properties to the final material [32]. The reported work proved that sorption of nickel ions was more effective when the polymer support was soluble in the media, which was possible as the copolymer was soluble at low temperatures. It was also demonstrated that the functional material enabled easy processing, since the polymer could precipitate at higher temperatures after the sorption step, without releasing the sorbed elements, allowing a facilitated separation of the nickel-sorbing polymer from the media, and an easy recovery/regeneration of the polymer and nickel ions. The authors also highlighted the influence of a copolymer architecture on its thermoresponsive properties [34]. Based on these works, copolymerizing a CE-bearing monomer and a monomer leading to thermoresponsive properties could constitute a promising material providing lithium-sorbing groups as well as easy post-sorption processing.

In the present contribution, we report the synthesis and use of original 12C4-containing copolymers with the aim to investigate its selectivity in LIB leachates (*i.e.* the aqueous acidic mixture of Li^+, Co^{2+}, Ni^{2+} and Mn^{2+} classically obtained at the beginning of the hydrometallurgy process). More particularly, we designed a CE-bearing monomer, namely 2-(benzo-12-crown-4-ether)ethyl methacrylamide (BCEEM), and synthesized it using two different pathways (from dopamine hydrochloride or from a commercial methacrylamide dopamine). Then, we copolymerized the BCEEM monomer with N-isopropylacrylamide (NiPAAm) at various ratios, to prepare original statistical copolymers with targeted thermoresponsive properties, in order to provide a better processability of our final adsorbing material. Sorption experiments were carried out varying different parameters of interest on copolymers showing the best compromise between a high proportion of CE complexing groups and appropriate LCST value minimizing heating to afford insolubility of cations/copolymer complexes. Competitive sorption experiments were finally performed, and the metal/polymer interactions were further understood from a thermodynamic and mechanistic point of view with Isothermal Titration Calorimetry and Dynamic Light Scattering measurements.

2. Experimental

2.1. Materials and methods

Dopamine methacrylamide (DMAAm) was purchased from Specific Polymers. Methacryloyl chloride was purchased from Merck, distilled and stored at -5 °C. Azobisisobutyronitrile (AIBN) was purchased from Merck and used after recrystallization twice in methanol. All the other mentioned chemicals and solvents were purchased from Merck and were used as received.

^{1}H NMR characterization of BCEEM from DMAAm was performed on a BRUKER Advance III - 600 MHz spectrometer, while the 2D NMR studies were performed on BRUKER Advance NEO - 400 MHz. LC-MS analyses were performed on a MicroTof QII mass spectrometer from Bruker, coupled with an Ultimate 3000 liquid chromatography system from Thermo Fisher Scientific. The ionisation source was positive Electrospray Ionization. Molecular weights of the polymers were determined by size exclusion chromatography (SEC) in DMF, in the presence of 0.1 wt% LiBr, at 60 °C with PMMA standards, with an RI detector. LCST measurements were performed on a Perkin Elmer Lambda 35 UV-Visible spectrometer equipped with a Peltier temperature programmer PTP-1 + 1 in Quartz cuvettes, at a selected wavelength of 700 nm. For LCST measurements in water, the transmittance through polymer solutions (20 mg in 5 mL Milli-Q water) was measured as a function of the temperature. The temperature ramp was 1 °C.min^{-1}, the transmittance was measured every 0.1 °C with a 0.01 °C precision, from 5 to 40 °C. The LCST was defined as the temperature for which the transmittance value reached 50 % with a 0.1 °C precision. To study the influence of lithium on the LCST of the polymer, polymer solutions (20 mg in 10 mL Milli-Q water) were mixed with small volumes of various concentrated lithium solutions a day before at 15 °C. The study aimed at varying initial lithium concentrations from 4 mM to 300 mM, corresponding to Li/CE ratios varying from 0.2 to 16. The temperature ramp was 0.5 °C.min^{-1}, the transmittance was measured every 0.2 °C with a 0.01°C precision, from 15 to 45 °C. Dynamic Light Scattering (DLS) experiments were performed on a Malvern Zetasizer Nano instrument, equipped with an integrated Peltier temperature control oven. A day prior to the analysis, all samples were prepared in polystyrene disposable cuvettes, at 15 °C, with a polymer concentration of 20 g.L^{-1} in water and lithium was added as a concentrated solution, in small volumes, so the polymer concentration did not vary. Three copolymer solutions were prepared: without lithium, in 8 mM of lithium and 300 mM of lithium (corresponding to Li/CE = 0.4 and 16, respectively). Temperature experiments were performed from 15 to 35 °C, with a temperature ramp of 0.5 °C.min^{-1}, the size was measured every 1 °C (with a precision of 0.1 °C), three times with a twenty times 10 s analysis program.

The lithium titration was performed on a Shimadzu ionic chromatography system, equipped with a Shim-pack IC-C1 column, at 40 °C. The mobile phase for the titration of monovalent ions (Li$^+$) was a solution of nitric acid (5 mM), flown at 1.5 mL.min^{-1} and the ions were detected by conductimetry. The titration of bivalent ions (Co^{2+}, Ni^{2+}, Mn^{2+}) by ionic chromatography (using the same column as for Li$^+$ ions) was conducted with a 0.15 M lactic acid mobile phase, with a pH of 3.35 (adjusted with sodium hydroxide), at a rate of 1.0 mL.min^{-1}. For the detection, a solution of 0.2 mM 4-(2-pyridylazo)resorcinol, 1 M acetic acid and 3 M ammonia was used as a post-column reagent (0.3 mL.min^{-1}) for a UV detection at 520 nm. The thermodynamic characterization and the interaction between the metal ions and the CEs of the copolymer were obtained from Isothermal Titration Calorimetry (ITC) at 25 °C with a TAM III multichannel calorimetric device equipped with a Micro Reaction System from TA Waters and dedicated nanocalorimeters. ITC experiments consisted in the periodic injection of 25 times 10 µL of an ionic solution, into an 800 µL cell containing the complexing functions (polymer), under mechanical stirring with a golden blade at 45 rpm. Each injection was spaced out by a 45-minute stabilizing period, and each experiment was performed as a simultaneous triplicate thanks to the presence of three independent nanocalorimetric systems. The effect of the dilution of the ionic solution into the 800 µL of water (without the polymer) was also determined in identical conditions, and subtracted to the measurements using NanoAnalyze Software. All ITC experiments were performed with metal nitrate solutions at 200 mM and polymer solutions of P(BCEEM-st-NiPAAm) 8/92 at 10 mg of polymer for 800 µL (7.4 mM of CE functions).

2.2. Synthesis of the crown ether-bearing monomer, namely 2-(benzo-12-crown-4-ether)ethyl methacrylamide (BCEEM)

General procedures for the synthesis of the monomer BCEEM are detailed in the Supporting Information.

2.3. General procedure for the synthesis of thermoresponsive poly(BCEEM-st-NiPAAm)

Copolymers containing various BCEEM/NiPAAm ratios were synthesized. All polymerizations were conducted in Schlenk round bottom flasks by free radical polymerization. For instance, the synthesis of P(BCEEM-st-NiPAAm) 13/87 is described here. BCEEM (0.30 g, 1.0 mmol), NiPAAm (0.70 g, 5.8 mmol), AIBN (10 mg, 0.06 mmol) and 1,4-dioxane (30 mL) were mixed and degassed by three freeze pump thaw cycles, and then heated at 70 °C for 24 h. The solvent was then removed under reduced pressure. The obtained solid was purified dissolving it in cold Milli-Q water (20 mL), and heating at 29 °C under magnetic stirring

yielding a rubbery texture. Purification procedure was carried out three times. Finally, the third precipitate was fully dried and crushed with a mortar and pestle to afford a brownish powder.

P(BCEEM-*st*-NiPAAm) 13/87:

^{1}H NMR (DMSO-*d₆*, 400 MHz): δ (ppm) 0.7-1.2 (m, H_b, $H_{d'}$), 1.3-1.6 (m, H_a, $H_{a'}$), 1.9-2.1 (m, $H_{b'}$), 2.65 (m, H_d), 3.35-3.45 (m, H_c), 3.5-4.1 (m, H_j, H_i, $H_{c'}$, H_h), 6.5-7.7 (m, H_e, H_f, H_g).

Size exclusion chromatography (eluent: DMF, standards: PMMA): M_n = 47 000 g.mol^{-1}; Đ = 2.26.

2.4. Preparation and titration of the metal solutions

Ionic solutions were prepared by dissolution of salts purchased from Thermoscientific (> 98% purity) in Milli-Q water (resistivity 18.2 MΩ.cm^{-1}. Although lithium chloride is often used in lithium adsorption studies, lithium nitrate was used by default for all the sorption experiments due to its lower toxicity and the best neutrality of the nitrate counterion. The lithium titration was performed by ionic chromatography. Additionally, to approach competitive adsorption in the context of LIB recycling, a multi-component solution was used, containing lithium nitrate, cobalt nitrate hexahydrate, nickel nitrate hexahydrate and manganese nitrate tetrahydrate. The concentrations resulted from the mean proportion of each ion in typical LIB leachates found in the literature [35-40]. The average concentrations were respectively 1.2 g/L, 7.8 g/L, 1.7 g/L and 2.0 g/L for Li$^+$, Co^{2+}, Ni^{2+} and Mn^{2+}. All these concentrations were divided by 30 to obtain experimental concentrations adapted to the laboratory scale, by preserving all metal/lithium molar ratios in the leachate. Additionally, three other intermediary conditions were tested (Table 1), to vary the Li$^+$/M molar ratio (M = Co^{2+}, Mn^{2+} or Ni^{2+}) for the same Li$^+$ concentration, from a solution where Li$^+$ is more concentrated than the other ions (Solution 1) to a solution where the molar concentrations of the four elements are closer (Solution 4).

Table 1

Typical multi-component solution compositions (mM) used for competitive sorption.

Solution	Li (mM)	Co (mM)	Ni (mM)	Mn (mM)
Solution 1	5.47	3.83	0.46	0.59
Leachate	5.47	4.25	0.92	1.19
Solution 3	5.47	4.65	2.44	2.62
Solution 4	5.47	5.1	4.0	4.1

As the pH of an ionic solution can greatly influence the adsorption capacity of a polymer, the same solution at various pHs was prepared. The use of nitric acid is described in the literature in industrial leaching steps as a leaching agent [41, 42]. Consequently, the acid and base used to adjust the pH were respectively nitric acid (to minimize the amount of counterions in the solutions) and triethylamine solutions. Triethylamine was chosen to ensure the absence of ionic base counterion representing potential competition to the metals of the study. To ensure that all metal salts were soluble at the pH and concentrations of the study, speciation diagrams were generated (see Supporting Information, Fig. S7 and Fig. S8) with Hydra database and Medusa software. For lithium alone, all the concentrations that were explored in this study showed full solubility at any pH. However, for the solutions containing cobalt, nickel and manganese, a pH higher than 8 involved a production of metal hydroxides that was too important, and subsequently the metals precipitated. As a consequence, all competition experiments were performed at pH = 7.

2.5. Sorption experiments

The sorption experiments were carried out in batch reactors. Dialysis membranes (Fisher Scientific Spectra/Por 6 tubular regenerated cellulose dialysis membrane with a molecular weight cut-off of 1 kDa) were used to ensure the absence of polymer compounds in the ionic chromatography samples. The thermoresponsive properties could have directly been exploited, however the influence of the precipitation on the Li/CE complex was initially unknown. The membranes were filled with 5 mL of a copolymer solution (20 to 80 g copolymer/L of milli-Q water) (See Supporting Information, Fig. S9). The membrane containing the copolymer solution was then placed into a cup containing 50 mL of a lithium solution (concentrations ranging from 0.05 to 3 mM). The cup was shaken at 180 rpm with a Stuart mini orbital shaker SSM1, installed inside an SH-641 Bench-top Type Temperature & Humidity Chamber from Espec programmed at a fixed temperature for a certain amount of time. The concentration of lithium in the outer solution before membrane immersion, after any time t of exposure and at equilibrium, was measured by ionic chromatography. The diffusion process of the lithium ions into the membrane was taken into consideration for the calculus of the polymer performances, by accurately weighing the volumes of each solution after pH adjustment.

Sorption kinetics. First, adsorption kinetic experiments were carried out to determine the equilibrium time to reach equilibrium adsorption capacity. Sorption kinetics were studied over 24 h by collecting ten times 100 μL samples, in order to keep the total initial volume (50 mL) change negligible (< 2 %). The lithium concentration outside the membrane at time t (C_t in mmol.L^{-1}) was used to monitor the kinetics.

Sorption isotherms. The influence of pH and temperature were studied, by performing a study at 5, 17, 25 or 35 °C at pH 9 for 24 h and at initial pH values of 3, 5, 7, 9 and 11 at 17 °C for 24 h. Then, lithium mono-component adsorption isotherms were performed at optimised pH (10) and temperature (17 °C), using batch reactors with the same initial polymer mass of 90 mg for 5 mL, and different initial lithium concentrations of 0.05, 0.1, 0.2, 0.8, 1.3, 2, 2.5, 3.3 and 5 mM. The lithium adsorption capacity of the polymer Q_e (mmol Li/mmol CE) was calculated from a mass balance:

$$Q_e(Li) = \frac{C_0 V_{Li} - C_e(V_{Li} + V_p)}{n}$$

where C_0 and C_e (mmol.L^{-1}) are respectively the concentrations of lithium outside the dialysis membrane initially and at equilibrium, V_{Li} and V_p (L) are the initial volumes of respectively the lithium solution and polymer solution after pH adjustment and n (mmol) is the number of moles of CEs inside the dialysis membrane.

Competitive sorption. The distribution of each adsorbed metal on the copolymer at equilibrium was calculated as follows:

$$D_M = \frac{Q_{ads}(M)}{\sum_i Q_{ads}(i)}$$

3. Synthesis and characterization of functional copolymers

3.1. Monomer synthesis

The CE-bearing monomer, namely the 2-(benzo-12-crown-4-ether)ethyl methacrylamide (BCEEM), was synthesized using two different reactional pathways (A and B), as shown in Fig. 1.
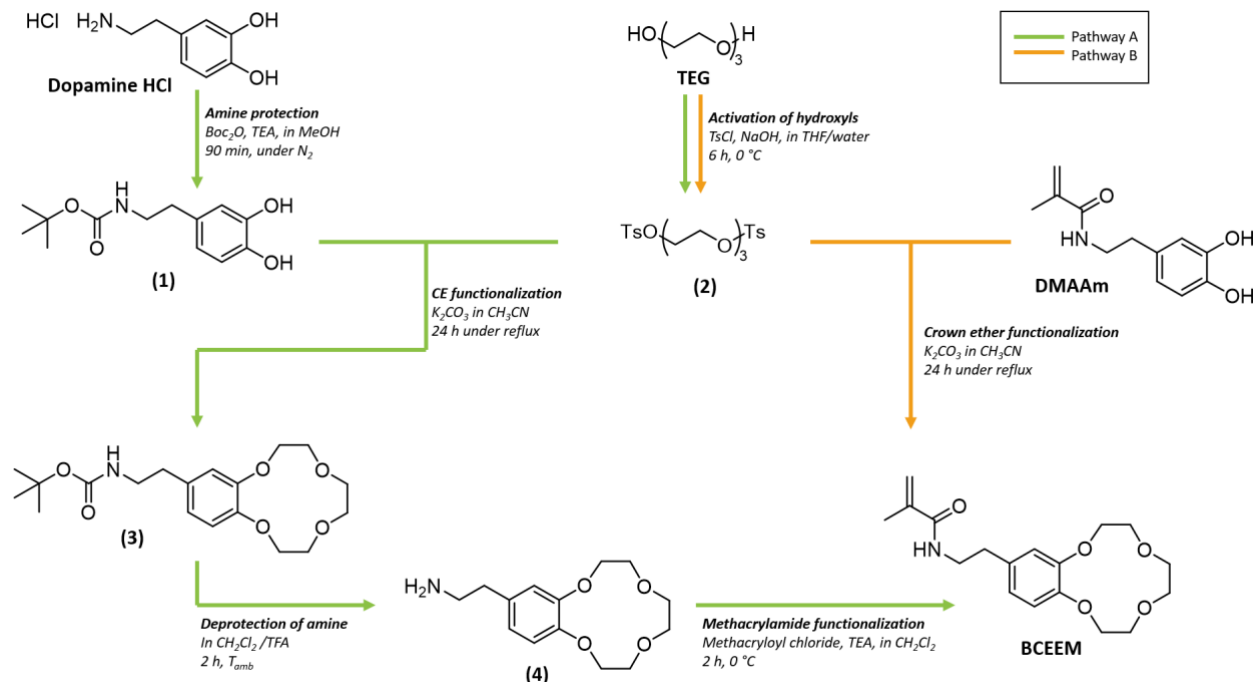
Fig. 1. Synthesis of the 2-(benzo-12-crown-4-ether)ethyl methacrylamide (BCEEM) monomer using two different pathways.

The first pathway A consisted in five steps, starting by the protection of the amine group of dopamine hydrochloride with a tertbutyloxycarbonyl (Boc) protecting group, resulting in compound **(1)**. The latter was prepared according to already known procedures with some modifications [13]. It was synthesized using an equimolar ratio of dopamine and di-tert-butyl-dicarbonate as excess of dicarbonate could generate the simultaneous protection of the amine and one of the two hydroxyl functions of dopamine. The ^{1}H NMR spectrum (see Supporting Information, Fig. S1) demonstrated that the reaction successfully occurred, notably with the appearance of the signals attributed to the methyls of the Boc group at 1.42 ppm. Additionally, the protection of the amine group was practically total. In parallel, the reactivity of triethylene glycol was improved by tosylating its hydroxyls groups, leading to compound **(2)**. The latter was synthesized using an excess of *p*-toluenesulfonyl chloride, (*i.e.* 1.1 eq) for each hydroxyl group instead of 0.6 eq per hydroxyl group as preconized in the literature [13]. This ensured a better activation of both end hydroxyl groups of the triethylene glycol, and improved the yield from 50 to 70%. Tosylated product was characterized by ^{1}H NMR (see Supporting Information, Fig. S2), with signals at 2.44, and 7.34 and 7.79

ppm, attributed to the methyl and the aromatic protons of the tosyl group, respectively. The, compound **(3)** was the result of the reaction of compounds **(1)** and **(2)** under reflux for 24 hours, forming a benzo-12-Crown-4-Ether from both hydroxyls of the dopamine compound. Purification was achieved by silica gel column chromatography using dichloromethane and methanol (90/10; v/v) to afford pure protected crown ether **(3)** as a brown solid with 79% yield. ^{1}H NMR in deuterated chloroform confirmed that the reaction was successful, notably with the protons attributed to the methyl groups at 1.43 ppm, the methylene groups of the crown ether function at 3.64, 3.66-3.78 and 4.02-4.12, and the aromatic protons at 6.67-6.81 ppm (see Supporting Information, Fig. S3). Then, the amine group was deprotected in the presence of trifluoroacetic acid (TFA) in dichloromethane leading to compound **(4)** in quantitative yield. Finally, compound **(4)** reacted with methacryloyl chloride, in the presence of triethylamine. Conversion of amine groups was equal to 90 % and the flash chromatography on silica gel column using dichloromethane and methanol (92/8; v/v) yielding pure 2-(benzo-12-crown-4-ether)ethyl methacrylamide (BCEEM) as a thick rusty orange paste in 55% yield. ^{1}H NMR in deuterated DMSO (Fig. 2) notably demonstrated the presence of methacrylamide polymerizable groups at 5.30 and 5.61 ppm, the presence of the methyl group at 1.83 ppm, methylene of the crown ether moiety at 3.62, 3.65-3.80, and 4.01-4.17 ppm, and the aromatic protons at 6.74-6.93 ppm.
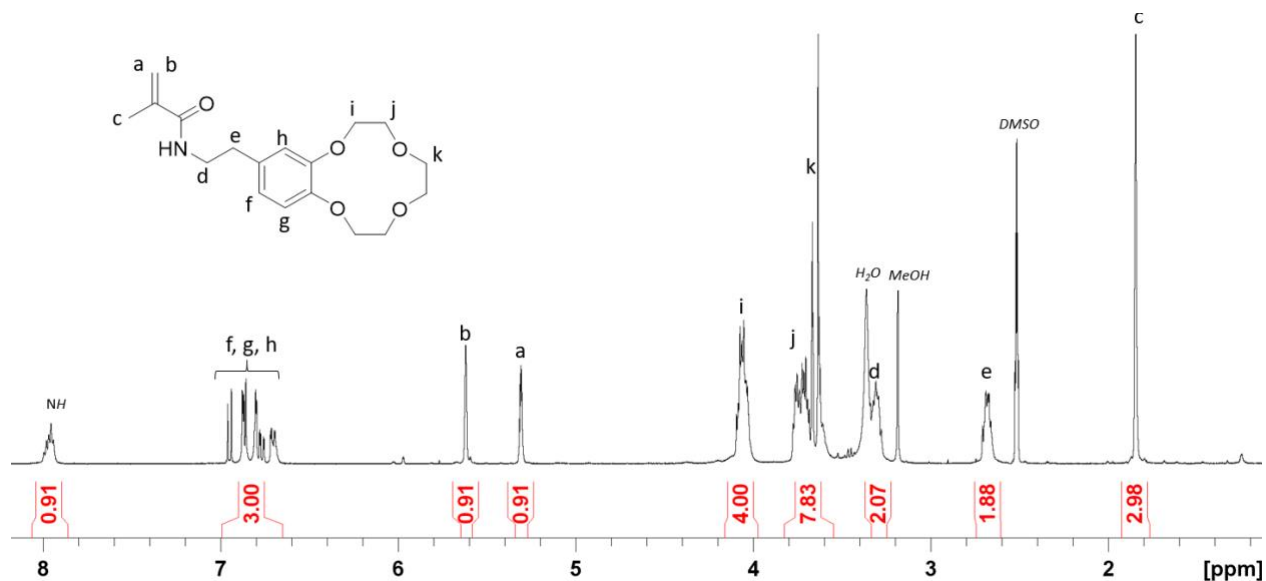

Fig. 2. ^{1}H NMR in DMSO-d_6 of the BCEEM monomer obtained from compound **(4)**.

BCEEM monomer was also prepared using a second pathway (pathway B), which was inspired from the synthesis of compound **(3)**, by reacting the ditosylated triethyleneglycol with an expensive commercially

available methacrylamide dopamine. Reaction was carried out in the presence of potassium carbonate in acetonitrile under reflux during 24 hours. After appropriate work-up, the crude material was purified by silica gel column chromatography using dichloromethane and methanol (92/8; v/v) to afford pure BCEEM as a thick rusty orange paste with 71% yield. The BCEEM monomer synthesized from DMAAm was characterized by ^{1}H NMR, which logically led to the same spectrum as the one for the BCEEM obtained with the synthesis from pathway A. This one has the advantage to enable the introduction of polymerizable groups of different chemical nature as a function of the last reactant employed (acrylamide, methacrylate, acrylate, etc.). From an industrial standpoint, despite pathway A also requiring cheaper reactants, pathway B offers more promising benefits. These include faster synthesis, improved yield, reduced need for reactants and solvents and a better global yield of 50 % compared to 28 % for pathway A. For these reasons, we used the BCEEM originating from pathway B for future syntheses. Nevertheless, a matter requiring thorough consideration for both pathways involve the simplification of some purification steps, given for example the inherent limitations of flash chromatography for industrial-scale applications.

3.2. Synthesis of copolymers

All copolymers were synthesized by free radical polymerization, wherein the molar ratio of BCEEM (prepared from dopamine methacrylamide) to NiPAAm (BCEEM/NiPAAm) was varied in the feed, ranging from 8/92 to 34/66 (Fig. 3). It is important to notice that higher proportions of BCEEM in the copolymer were also considered but resulting materials proved not to be thermosensitive and insoluble in water. As a result, they were not further considered. Copolymerizations were carried out in 1,4-dioxane, under nitrogen in the presence of AIBN at 70 °C during 24 hours.
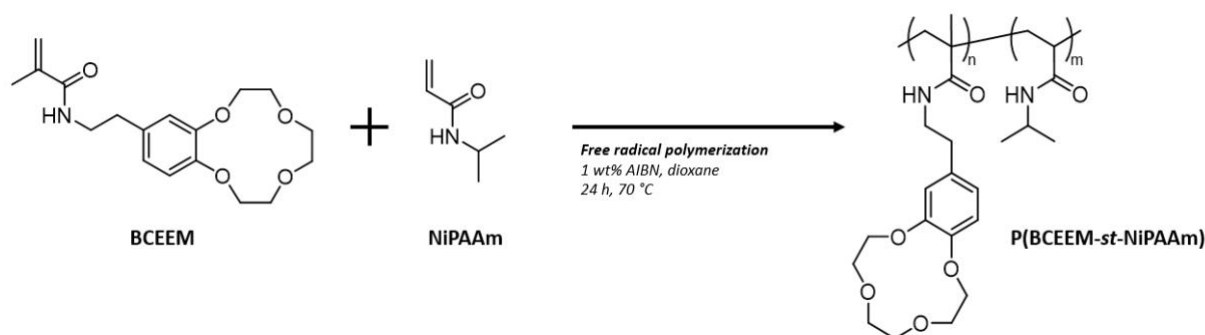

Fig. 3. General polymerization reaction allowing the synthesis of P(BCEEM-*st*-NiPAAm) statistical copolymers.

Conversion was measured comparing polymerizable groups of BCEEM and NiPAAm to i) the aromatic groups of BCEEM which where present in both the monomer and the copolymer and ii) the apparition of the CH in the polymer backbone for NiPAAm. For all copolymers, both monomers reached a conversion around 90 %. After evaporation of the solvent, ^{1}H DOSY NMR study of the crude material (Fig. S4) demonstrated that poly(N-isopropyl acrylamide) (P(NiPAAm)) was also synthesized, as NiPAAm was used in relatively large excess. As Lower Critical Solution Temperature (LCST) of P(NiPAAm) homopolymer was measured at 31 °C (Fig. 5) and as LCST of the copolymers was necessarily lower than the one of P(NiPAAm), due to hydrophobic character of BCEEM moieties, we ensured the correct purification of the copolymers by selectively precipitating them at a temperature between both LCSTs. So crude material was dissolved in Milli-Q water and the resulting solution was heated up to 29 °C. In a general manner, when LCST of the copolymer was reached, the latter became insoluble in water (whereas P(NiPAAM) was still soluble in water) and was recovered by filtration as a brownish powder. ^{1}H DOSY NMR of the purified copolymers (Fig. S5) confirmed the efficiency of the purification step, as the diffusion coefficient corresponding to the monomers and the P(NiPAAm) homopolymer had disappeared. Obtained yields were medium (up to 45 %) as some copolymers were obviously lost during the precipitation. Nevertheless, the developed purification procedure was kept, as it was simple to carry out and allowed the obtaining of pure materials, which was essential for an accurate determination of sorption properties. ^{1}H NMR spectrum of the copolymers (Fig. 4) showed signals corresponding to both BCEEM and NiPAAm moieties, in particular aromatic protons at 6.5-7.7 ppm and CH of the polymeric backbone at 1.9-2.1 ppm, respectively.
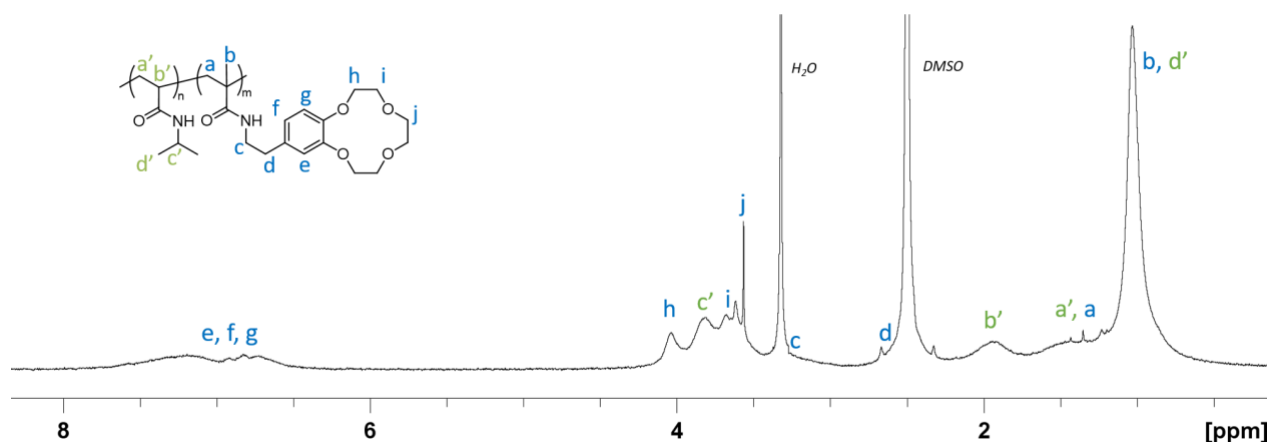

Fig. 4. ^{1}H NMR in DMSO-d_6 of the synthesized P(BCEEM-*st*-NiPAAm) 13/87.

Copolymers were synthesized on a scale of 1 to 10 g, their final compositions were determined by ^{1}H NMR spectroscopy (Table 2) by comparing signals at 3.9-4.1 ppm corresponding to the four protons of the crown ether closest to the aromatic group (H_h), or the three protons of the aromatic group (H_e, H_f, H_g), with the signal of the CH of NiPAAm ($H_{b'}$) belonging to the polymer backbone.

Table 2

Characterization of P(BCEEM-*st*-NiPAAm) copolymers.

Polymer name	Initial feed (BCEEM/NiPAAm)[a]	Final feed (BCEEM/NiPAAm)[a]	M_n[b] (g.mol^{-1})	$Đ$[b]
P(NiPAM)	0/100	-	38 000	1.81
P(BCEEM-*st*-NiPAAm) 8/92	8/92	7/93	71 000	1.82
P(BCEEM-*st*-NiPAAm) 13/87	13/87	14/86	47 000	2.26
P(BCEE-*st*-NiPAAm) 25/75	25/75	26/74	110 000	2.37
P(BCEE-*st*-NiPAAm) 34/66	34/66	36/64	14 000	2.87
P(BCEEM)	100/0	-	56 000	1.88

[a] Initial feed and final feed in mol/mol; [b] determined by size exclusion chromatography (eluent: DMF, standards: PMMA).

Size exclusion chromatography (SEC) using PMMA standards allowed the determination of molecular weights and dispersities ($Đ$) according to PMMA standards (Table 2). For simplicity, syntheses were achieved keeping the same global masses of monomers (typically 1 gram) and of initiator (1 % by weight) for all initial feeds. As a consequence, obtained copolymer molecular weights (M_n) were different (from 14 000 to 110 000 g.mol^{-1}). This difference of M_n was taken in consideration for sorption experiments, as sorption capacities were expressed as a function of mmol of complexing groups. Finally, reactivity ratios of BCEEM and NiPAAm in the copolymer were calculated using Jaacks method (see Supporting information, Fig. S6) [43] in order to have a more accurate idea of the copolymer architecture. It was found that r_{BCEEM} was slightly higher than 1 (r_{BCEEM} = 1.29), indicating that BCEEM radicals slightly preferred to react with another BCEEM monomer than with NiPAAm; and r_{NiPAAm} was slightly lower than 1 (r_{NiPAAm} = 0.86), indicating that a NiPAAm radical slightly preferentially reacted with BCEEM monomers. Architecturally, this means that along the copolymer chain, the distribution of both monomers is not fully

statistical, but rather presented areas with high proportions of BCEEM and others with high NiPAAm moieties content. This architecture is of interest as the gathering of the NiPAAm thermoresponsive segments favours the thermoresponsiveness of the copolymers [34].

This range of copolymers, with varying BCEEM/NiPAAm monomer ratio ranging from 8/92 to 34/66 was studied to identify the optimal composition in terms of highest content of CE moieties while keeping LCST close to room temperature in order to minimize the energetic impact while heating from soluble to insoluble state for the copolymer. Determination of thermosensitive properties was accurately carried out to identify chemical polymeric structure allowing the best compromise. It is worth mentioning that, in a general manner, molecular weights of polymers proved to have no influence on the LCST values, which remain constant whatever the molar mass, in particular in the case of poly(N-isopropylacrylamide) [44].

3.3. Thermoresponsive properties of the copolymers

The influence of the NiPAAm/BCEEM ratio on the LCST of the copolymer was determined by measuring the transmittance of polymer solutions as a function of the temperature (Fig. 5). First, the results demonstrated that with an increasing proportion of BCEEM monomers, the LCST of the copolymer decreases, which is coherent due to the hydrophobic nature of BCEEM (Fig. 5a). Indeed, hydrophobic components acted as a hindrance to the hydrogen bonding of the NiPAAm groups with water. Consequently, with an increased proportion of BCEEM, less thermal energy was necessary to break the remaining water-polymer interactions before the polymer only interacted with itself. As a result, the LCST was lower. With BCEEM/NiPAAm molar ratios ranging from 8/92 to 34/66, the LCST varied from 6.2 to 26.5 °C, where 6.2 °C was the lowest LCST we reached with the highest proportion of BCEEM. For even higher proportions of BCEEM, the copolymer was simply no longer soluble in water, no matter the temperature. The behaviour of our copolymers in relation to their composition and their architecture was in accordance with the literature [34]. At a macroscopic level, functional copolymers clearly precipitated in water (Fig. 5b), which is a key point leading to an easy filtration of the materials after the sorption of cations of interest.
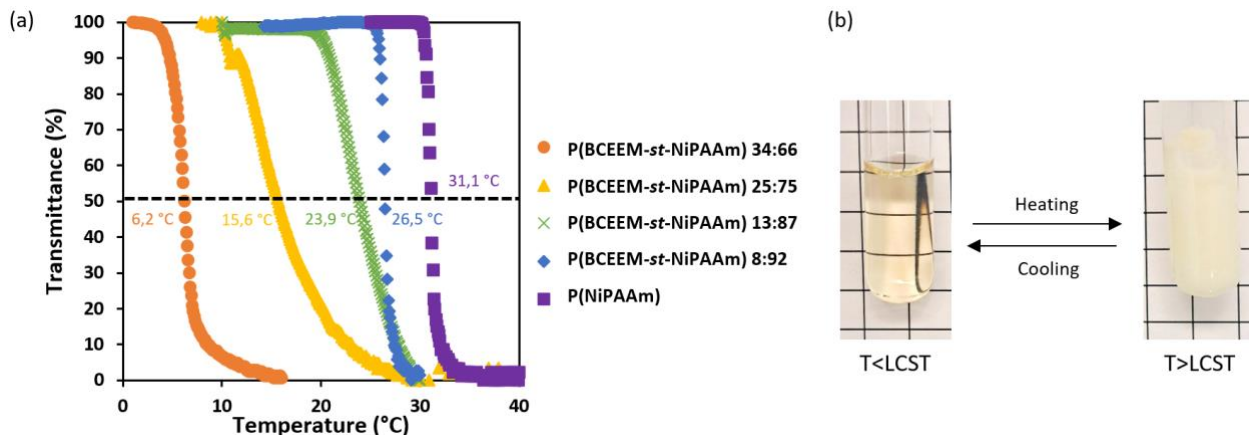
Fig. 5. a) Evolution of the LCST of P(BCEEM-*st*-NiPAAm) with the variation of BCEEM/NiPAAm molar ratio in the copolymer and b) visual aspect of the P(BCEEM-*st*-NiPAAm) 13/87 in water at 10 and 40 °C.

The objective of the reported work was to target a LCST close to room temperature in order to minimize heating energy requirements (around 24 °C). As a result, BCEEM/NiPAAm ratio equal to 13/87 was selected for the following sorption studies, as it features the highest density of BCEEM functions, while providing the LCST closest to room temperature.

4. Sorption experiments

4.1. Sorption kinetics

Since crown ethers are most known for their affinity towards lithium ions, in processes involving liquid-liquid or liquid solid extractions, preliminary experiments aimed at evaluating the sorption efficiency of the copolymer at soluble state, in homogeneous solutions only containing lithium. The sorption kinetics of lithium (initial concentration of 1.85 mM) onto P(BCEEM-*st*-NiPAAm) 13/87 in our dialysis configuration at 180 rpm (see Supporting Information, Fig. S9) were evaluated over three days in order to determine the equilibrium time. According to the kinetic curve (Fig. 6), the amount of lithium sorbed onto the polymer reached an equilibrium concentration C_e of 1.56 mM after around seven hours, corresponding to an equilibrium adsorption capacity of 0.074 mmol/mmol CE (corresponding to 0.088 mmol/g polymer). However, this duration does not only represent the time for lithium sorption onto the polymer, but also the diffusion time of lithium ions through the membrane. This diffusion time through the membrane was

determined for experiments without polymer and a diffusion time of approximately 2 h was found. Taken this into consideration, we decided to conduct all adsorption evaluations after 24 h of membrane immersion.
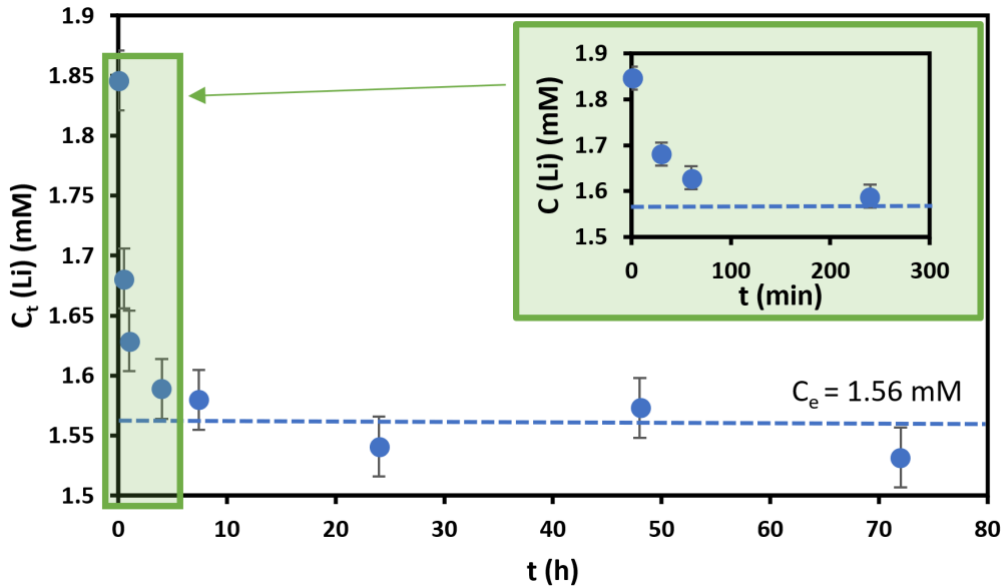

Fig. 6. Evolution of the concentration of lithium outside the dialysis membrane over 3 days with P(BCEEM-*st*-NiPAAm) 13/87 at pH_0 = 10, T = 17 °C, C_0 = 1.8 mM, [CE] = 15 mM and Li/CE = 1.3.

4.2. Influence of the pH

Several studies have reported the influence of pH on the sorption capacity of lithium by CEs complexation functions [25, 45, 46]. The main finding of these studies was that the optimal pH for adsorption ranges from 6 to 9. At higher pH levels, sorption capacities may slightly decrease, but no further explanation is provided in the literature. Meanwhile, at a lower pH, the concentration of protons becomes non negligible, and since protons are smaller in size than lithium ions, they will take the place of lithium ions, causing lower lithium adsorption capacities. In fact, this property is used to perform desorption steps for the regeneration of the CEs. The influence of pH on the adsorption capacity of P(BCEEM-*st*-NiPAAm) 13/87 was observed by studying the complexation of lithium ions at pH 3, 5, 7, 9 and 11. The results (Fig. 7), indicate that the adsorption capacity of the copolymer at a fixed Li/CE ratio was not significantly dependant of the pH, as the adsorption capacity ranged from 0.035 to 0.045 mmol/mmol CE

(corresponding to 0.04 to 0.06 mmol Li.g^{-1}) with no particular tendency compared to the standard deviation. Additionally, no variation in pH was observed at equilibrium compared to the initially adjusted pH, which refutes a possible ion exchange mechanism hypothesis. Thus, for future adsorption experiments, the working pH was adjusted to 7 or above, accordingly to the literature to ensure comparable parameters. However, as mentioned earlier, multi-component experiments were performed at a pH not higher than 7 following speciation to avoid precipitation.
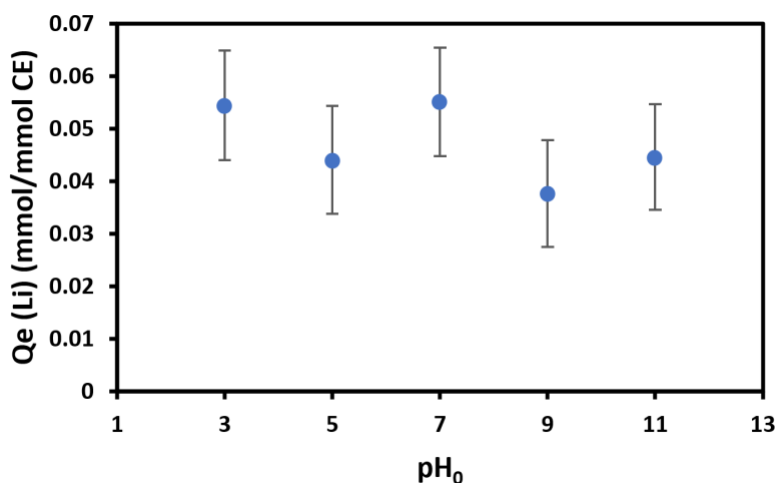

Fig. 7. Variation of the Li sorption capacity as a function of the initial pH, obtained with P(BCEEM-*st*-NiPAAm) 13/87 at 17 °C, after 24 h, C_0(Li) = 5.5 mM, [CE] = 11 mM and Li/CE = 2.

4.3. Influence of the temperature

By subjecting the adsorption of lithium onto P(BCEEM-*st*-NiPAAm) 13/87 to a range of temperatures, spanning from 5 to 35 °C, we investigated how changes in temperature influenced the adsorption capacity of the polymer for lithium (Fig. 8a), in relationship with the evolution of the LCST (Fig. 8b) and the size of the copolymer in the presence of lithium (Fig. 8c).
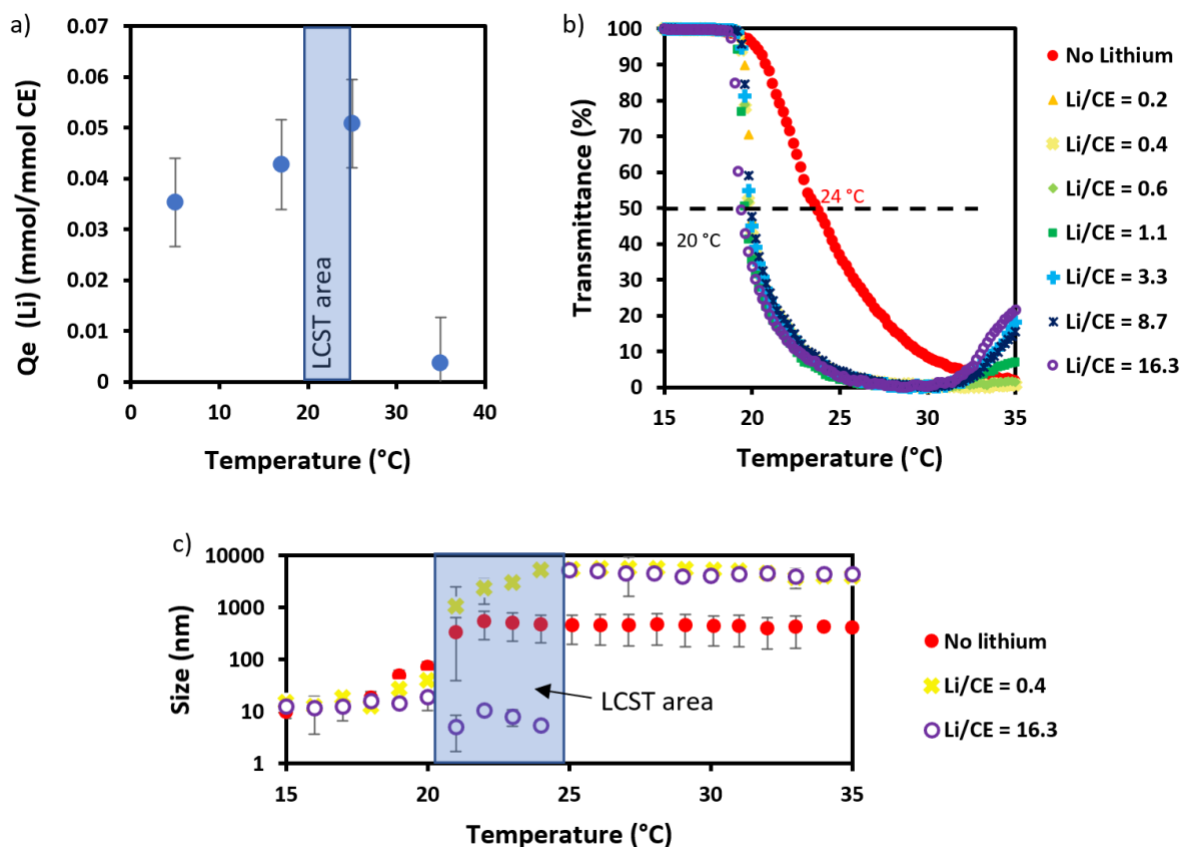
Fig. 8. Influence of a) the temperature on the adsorption capacity of P(BCEEM-*st*-NiPAAm) 13/87 at pH_0 = 9, t = 24 h, $C_0(Li)$ = 1.8 mM, [CE] = 30 mM and Li/CE = 0.6, b) the presence of lithium on the LCST of the copolymer Li/CE varying from 0.2 to 16.3 and c) the presence of lithium on the polymer size as a function of temperature.

First, it is important to note that an LCST area was defined as the temperature range for which the polymer/polymer interactions start to prevail over polymer/solvent interactions, in the presence of lithium. This area appears narrow according to UV-vis measurements, as shown in Fig. 8b, where the transmittance of the polymer/lithium solution shifts rapidly, around 20 °C, no matter the Li/CE ratio. However, temperature-dependant DLS measurements, shown in Fig. 8c, indicated that this LCST area can be widened, as the agglomeration of the polymer in the presence of lithium (initial Li/CE ratio ranging from 0.4 to 16.3) necessitated a temperature range from 20 to 25 °C.

According to the literature, in the case of thermoresponsive copolymers bearing crown ethers, the addition of ionic species should induce a shift of the LCST towards higher values. This phenomenon is called

salting-in effect: the bound cations increase the hydrophilicity of the CEs by promoting interactions between the polymer and water [47-50]. However, the opposite behaviour was observed with P(BCEEM-st-NiPAAm) 13/87, indicating a salting-out effect, rather reinforcing polymer/polymer interactions, due to potential interactions of the available lithium ions with water molecules that were involved in hydrogen bonding with the heteroatoms of the polymer [51]. This hypothesis was reinforced by the DLS measurements in Fig. 8c. At temperatures below the LCST area, the size of the polymer in water was around 10 nm without or with lithium. However, above the LCST area, while the polymer without lithium reached an aggregated conformation size of 500 nm, the size of the same polymer in the presence of lithium increased to reach sizes 10 times bigger (5 µm) no matter the concentration of lithium. This higher size may be indicative of stronger interactions of the polymer with itself and a more rigid conformation. Moreover, the reason for this salting-out effect may be the consequence of too weak interactions between the CEs and lithium, resulting in the low amount of ions in the CE cavities. This could also explain the quite low adsorption capacities observed in the overall study and was further verified by ITC measurements for a thermodynamic understanding at the end of this study.

These observations can be correlated to the equilibrium sorption capacities obtained for Li/CE = 0.6 at different temperatures around the LCST area (5, 17, 25 and 35 °C) (Fig. 8a). A maximum sorption capacity of 0.05 mmol Li/mmol CE was observed at the temperature close to the LCST area (25 °C). This value was obtained for a copolymer initially partially soluble within the dialysis membrane (because the operating temperature was close to its LCST, the solution was visually cloudy), leaving the CEs available for lithium complexation. As the Li$^+$ ions gradually diffused through the dialysis membrane, the precipitation of the polymer became more pronounced as its LCST decreased towards a value of 20 °C (increasing the deviation from the experimental temperature), causing the complete precipitation of the polymer. At temperatures below the LCST area, an increase in temperature improved the sorption capacity of the fully soluble polymer from 0.035 to 0.05 mmol Li/mmol CE (corresponding to 0.04 to 0.05 mmol Li.g^{-1}). This may be explained by a better diffusion of Li$^+$ towards the CEs at higher temperatures due to an increased entropy. However, at temperatures above the LCST, as the copolymer favored polymer-polymer interactions, it fully precipitated. Visually, the polymer regrouped into a ball, making the CE sorption sites unavailable, hence a drastically dropping sorption capacity to almost 0 mmol Li/mmol CE. This general trend is in accordance with the literature [32, 52], and is even observed in non thermoresponsive materials, which is explained by a too elevated entropic contribution. Finally, to avoid any confusion with the evolution of the LCST in the presence of lithium, all sorption experiments were conducted at 17 °C.

On a final note, further investigations showed that any Qe obtained after 24 h of membrane immersion at 17 °C did not vary after heating the membrane at 35 °C for an extra 24 hours, indicating that post sorption separation by precipitation did not affect the amount of lithium that was recovered (see Supporting Information, Fig. S10).

4.4. Sorption isotherm

After optimizing the pH and temperature, we proceeded to investigate the sorption isotherm of lithium onto our synthesized material (pH = 7, T = 17 °C, stirring equilibrium time = 24 h). The study sought to elucidate the maximum experimental sorption capacity of the material by keeping constant the mass of polymer, and varying the initial feed composition ([Li$^+$] varying from 0.05 to 5 mmol.L^{-1}), to obtain the sorption isotherm (Fig. 9a).
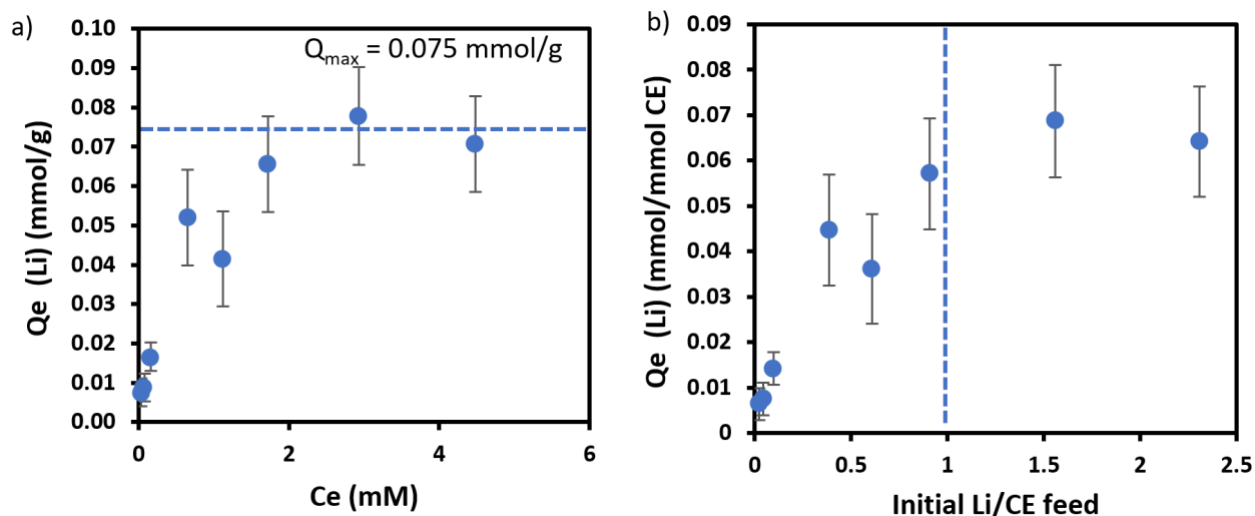

Fig. 9. Lithium a) sorption isotherm and b) sorption capacity relatively to the initial molar ratio Li/CE, with P(BCEEM-*st*-NiPAAm) 13/87 at pH$_0$ = 10, T = 17 °C, t = 24 h, C$_0$(Li) varying from 0.05 mM to 5 mM and [CE] = 22 mM.

Adsorption capacities may be expressed as the molar ratio sorbed Li/CE as a function of the initial Li/CE molar ratio (Fig. 9b) to yield an adsorption isotherm exhibiting two distinct phases that are more interpretable from a more mechanistical point of view. On the one hand, in a molar excess of CEs compared to lithium (Li/CE < 1), the lithium adsorption capacity increased linearly with the increase of

initial Li$^+$ ion concentration, from 0.006 to 0.060 mmol/mmol. This indicated that the driving force behind the lithium/CE adsorption was generated by the simple gradient of lithium concentration. On the other hand, when the molar ratio Li/CE exceeded the value of 1, the adsorption capacity plateaued at a maximum adsorption capacity of Q_{max} = 0.07 mmol/mmol, implying that the complexing sites of the copolymer may have reached a certain level of saturation. Yet, this Q_{max} value seems rather surprising compared to the available CE sites in the medium. For instance, with an initial feed of 3 Li$^+$ ions for 2 CE groups, it means that only 0.07 mmol of ions per CE were reportedly sorbed. This may be due to intrinsic properties of the copolymer itself, and its macroscopic interaction with lithium was further verified by ITC measurements. When expressed relatively to the mass of polymer, the maximum adsorption capacity of 0.075 mmol/g polymer (= 0.55 mg.g^{-1}) falls at the lower end of the typical range reported in the literature for the complexation of lithium with CEs (12-crown-4 or 14-crown-4 ethers), which mostly spans from 14.6 µg.g^{-1} to 27 mg.g^{-1}. However, these findings are challenging to reconcile with existing literature, given the prevalence of water-insoluble systems such as membranes [28, 45, 53], foams [27], insoluble particles [25, 52, 54, 55], microfibers [14, 56], nanostructures [26, 46], gels [19] or exchange resins [24]. Additionally, there is a limited availability of CE density data, and instead of Li/CE ratios, only material mass compared to ion concentrations are given. Notably, in our case, the copolymer is loaded with only 13 mol% of sorbing functions, as dictated by our LCST properties. CE-denser systems would require less polymer to achieve similar results, thus potentially yielding higher sorption values in mg.g^{-1}.

4.5. Competitive sorption in leachate conditions

In addition to the study of lithium adsorption capacity of P(BCEEM-*st*-NiPAAm) 13/87, we investigated the potential selectivity that the CEs could provide towards lithium, accordingly to the literature. Not only did we investigate the competitive sorption in typical synthetic leachates originating from the LIB recycling industry (typically composed of mostly Li and Co, and lower amounts of Ni and Mn), but we also wanted to evaluate the selectivity in intermediary scenarios, as described in Table 1. Li$^+$ concentration was fixed for all solutions while other ion concentrations were increased from solution 1 (Li$^+$ concentration higher than other ion concentrations), solution 2 (leachate concentration ratio), solution 3 up to solution 4 (Li$^+$ concentration close to other ion concentrations). Fig. 10a illustrates the ion adsorption capacity of the thermoresponsive copolymer at soluble state for solution 1, leachate, solution 3 and solution 4 conditions, as well as the distribution of ions among the adsorbed ions at equilibrium. For instance, the distribution

of sorbed lithium ions was calculated by dividing the moles of sorbed lithium ions by the total molar sum of sorbed metal ions.
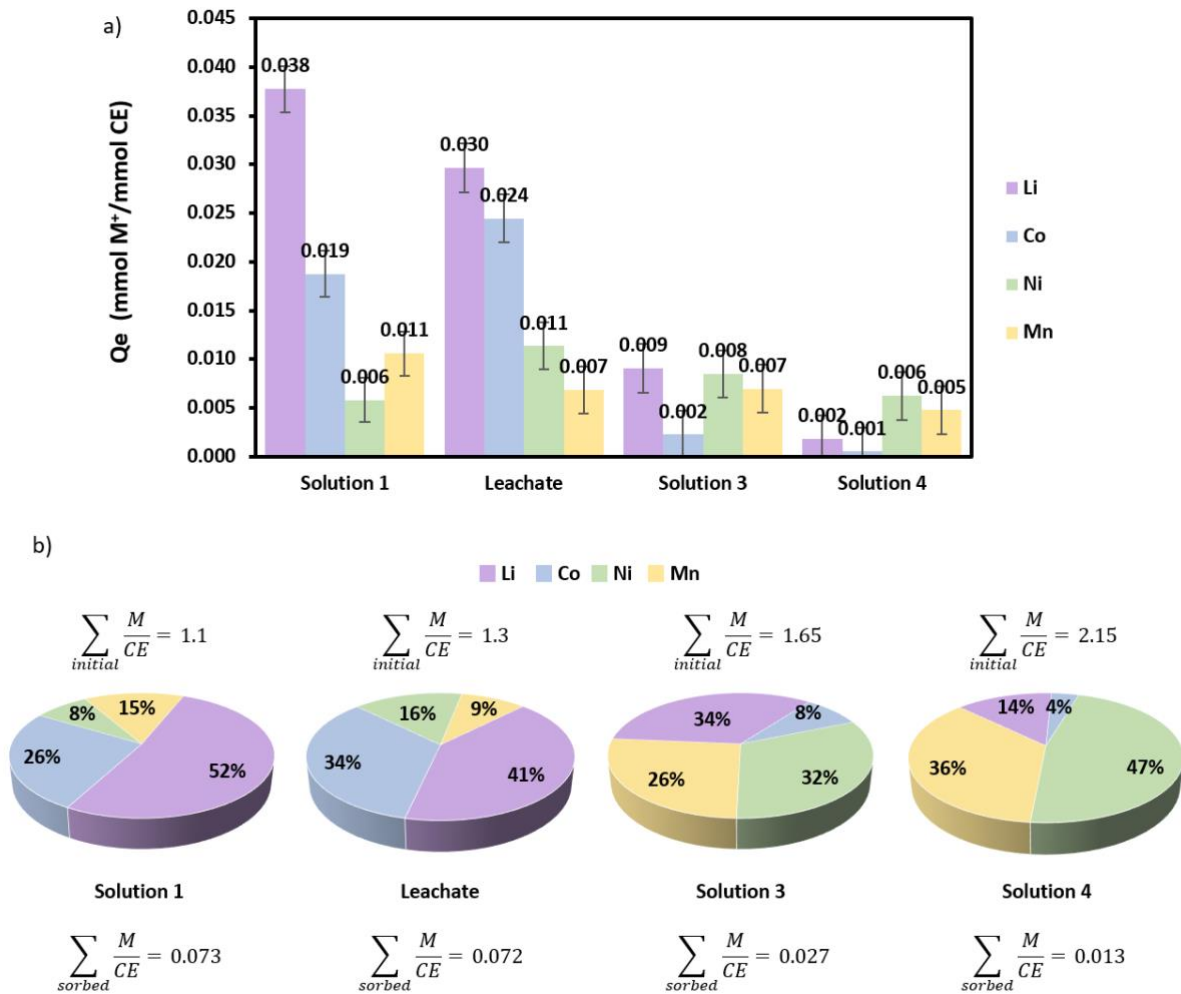

Fig. 10. a) Ion sorption capacity of P(BCEEM-*st*-NiPAAm) 13/87 in the multi-component solutions, at $pH_0 = 7$, $T = 17\ °C$, $t = 24\ h$ and $[CE] = 88\ mM$ and b) ion distribution among the sorbed ions on the polymer as a function of initial molar Metal/CE feed and resulting total adsorbed Metal/CE ratio.

The trend observed in Fig. 10b shows that in the presence of multi-elements, with the increasing initial M/CE ratio (*i.e.*, increased ion concentration), the total ratio of sorbed ions per functional group drastically decreased from 0.073 to 0.013. It is worthfully to notice that separation factors were also determined and led to similar tendencies. Cobalt, nickel and manganese are bivalent cations which present respectively 9.6, 10.4 and 8.7 water molecules immobilized around them, compared to only 5.2 for lithium [57].

Consequently, increasing the concentration of bivalent ions may cause increased interactions of the metals with water, and thus decreased interactions between the water molecules and the polymer, *i.e.*, the salting-out effect above-mentioned. A second trend resulting from the competition study is that in leachate-type solutions (Solution 1 and leachate being very close in composition, with an excess of Li^+ and Co^{2+}), the copolymer showed selectivity towards lithium and cobalt, with a total loading of 75 % corresponding to only those two ions. However, when increasing the proportions of bivalent ions (Solutions 3 and 4), the more Ni^{2+} and Mn^{2+} ions were preferred, with a total loading of 83 % for only these two ions in Solution 4. This may be attributed to different affinities between the CE and the different metals, and it was verified with thermodynamic data obtained from ITC.

4.6. Isothermal Titration Calorimetry

To better understand the sorption capacities of the polymer and its solution-dependant selectivity, Isothermal Titration Calorimetry (ITC) measurements were performed to determine the single-ion thermodynamic interactions between lithium, cobalt, nickel and manganese with the CEs supported by the copolymer. The copolymer used for this study was P(BCEEM-*st*-NiPAAm) 8/92 (Fig. 5, LCST = 26.5 °C) as we worked at a temperature equal to 25 °C, which was superior to the LCST of P(BCEEM-*st*-NiPAAm) 13/87 (Fig. 5, LCST = 23.9 °C). Here, we ensured that the polymer was fully soluble at 25 °C. An example of the obtained ITC thermograph and titration curve for lithium is shown in Fig. 11 (see Supporting Information Fig. S11-S13 for other single-ion ITC curves with Co, Ni and Mn).
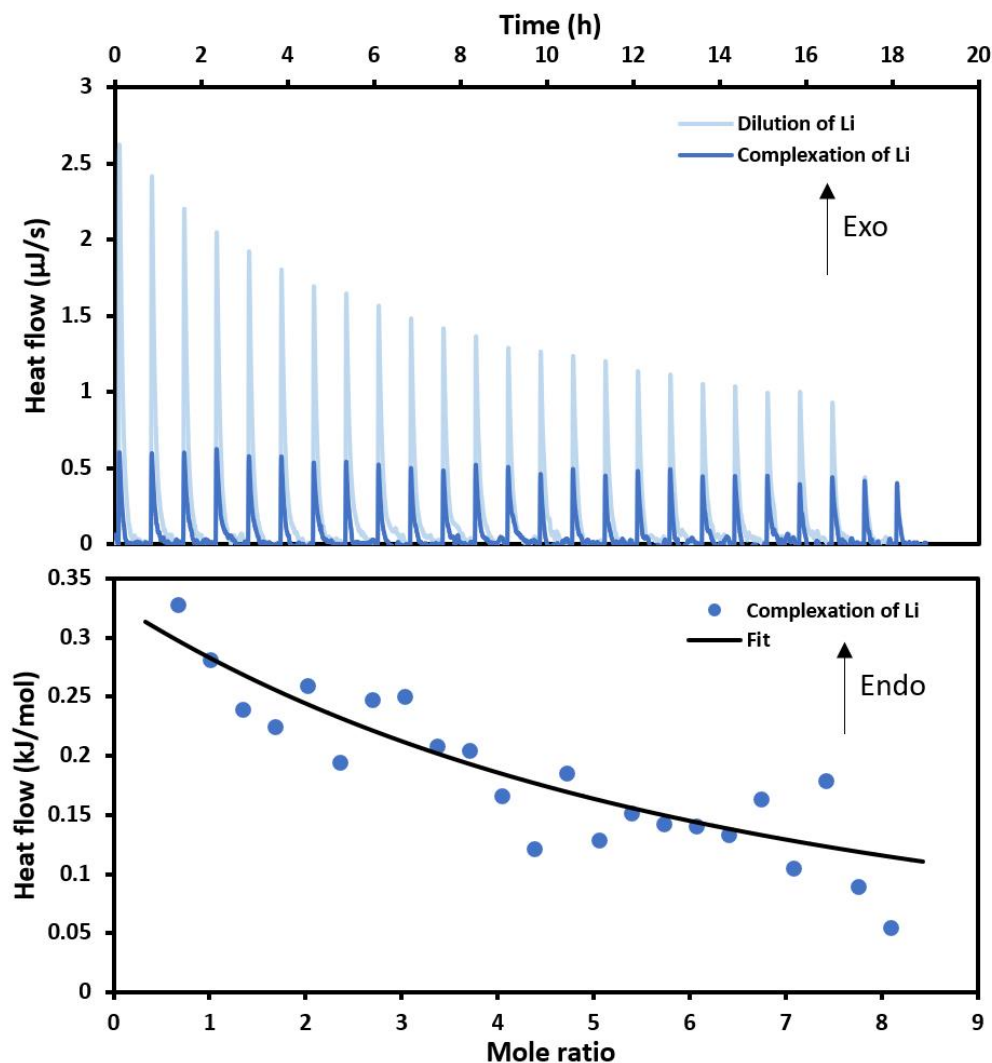
Fig. 11. Example of ITC thermograph (top) and titration curve (bottom) corresponding to P(BCEEM-*st*-NiPAAm) 8/92 with lithium nitrate ([Li⁺] = 200 mM, 10 mg of polymer for 800 µL).

In Fig. 11 (top), the dark blue peaks corresponding to the complexation of lithium were exothermic, with a quite constant heat rate of 1 µJ.s⁻¹ for each injection. Similarly, the light blue peaks describing the dilution of lithium at the same concentration, into water only, also presented exothermic peaks. Fitting of the titration curve (Fig. 11 (bottom)) with an independent model (confidence 95 %) provided information on thermodynamics constants relative to the complexation of lithium onto our P(BCEEM-*st*-NiPAAm) 8/92, such as the dissociation constant (K_d), stoichiometry (n), or enthalpy (ΔH). Although the obtained data was of good quality, the fitting of the curves was challenging due to very low variations in the titration curve,

no matter the initial molar ratio between the CE functions in the cell and total injected lithium. Consequently, the determination of n and ΔH was uninterpretable. In the case of lithium specifically, the K_d values that were extracted from the fitting curve were weak. In the end, the mean association constants obtained for our copolymer with Li^+, Co^{2+}, Ni^{2+} and Mn^{2+} in mono-element conditions were summarized in Fig. 12.
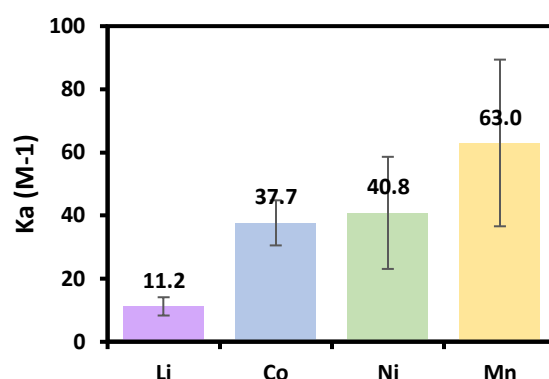

Fig. 12. Binding constants of P(BCEEM-*st*-NiPAAm) 8/92 with lithium, cobalt, nickel and manganese obtained by ITC.

First, in the case of lithium, the mean K_d for three measurements ranged at 0.09 M, *i.e.* an association constant of 11 M^{-1}. This illustrates the global weak association of lithium with the CEs of the copolymer compared to the literature. Luo et al. compared 12C4-bearing liquid crystalline receptors in recovering lithium through liquid-liquid extractions. They investigated the influence of a benzene group on the complexing efficiency (CE) by comparing the association constants of lithium with a 12C4 derivative and a similar benzo-12C4 derivative. While the 12C4 derivative had a binding constant of 610 M^{-1}, the benzo version showed a much lower value of 36 M^{-1}, which is similar to our findings. They attributed these findings to the rigidity of the benzo group, which reduces the flexibility of the receptor and as a consequence the availability of the CEs. Concerning the other ions, the binding constants of the polymer with cobalt, nickel and manganese were respectively 38, 41 and 63 M^{-1}, which was slightly higher than for lithium. This was in accordance with the observations made for the competitive experiments that showed that the higher the excess of bivalent ions, the more the polymer was selective towards them. Nevertheless, the binding constants remained quite low compared to reported Ka constants determined by NMR in the literature for similar systems [58, 59]. A possible reason for this is once again the number of water molecules immobilized around the ionic species when in solution [57]. This difference is naturally

linked to the bivalence of the latter. However, it also suggests that ions accompanied by a large hydration sphere, potentially available for complexation, are repelled by the rigid and hydrophobic aromatic groups adjacent to the complexing functions. Possible improvements could consist in using a larger crown ether group (such as 14C4, for instance) or using an open ether form moiety such as an ethylene glycol oligomer.

A final discussion was focused on the selectivity of the polymer towards cobalt and especially lithium in leachate-like solutions, although lithium has the smallest affinity with the CEs of the material. It is important to note that the polymers used for batch sorption process and for ITC were slightly different in composition (BCEEM/NiPAAm ratio of either 8/90 or 13/87). Additionally, the Ka values obtained from ITC do not reflect the behaviour of the polymer in a competitive scenario: it can only help understand the individual single-ion interaction between each ion and the polymer. As a consequence, the highest sorption capacity attributed to lithium in solution 1 may be caused by differences in initial concentrations: saturating the solution with lithium and cobalt compared to the other species (as ruled by the leachate composition), may help force the sorption of both elements.

5. Conclusion

In conclusion, the present contribution has focused on the development of new valuable functional polymers for the sorption of lithium. First, the successful synthesis of a novel CE-bearing monomer was achieved through two synthetic pathways. The optimal pathway to synthesize BCEEM involved the addition of a ditosylated TEG onto a commercial methacrylamide-functionalized dopamine. A faster synthesis, an improved yield, a reduced quantity of reactants and solvents, and a cost-effective synthesis are the main highlights of this pathway. Then, different free radical copolymerization of BCEEM with NiPAAm successfully yielded a wide range of thermoresponsive P(BCEEM-*st*-NiPAAm) polymers with targetable BCEEEM/NiPAAm ratios and LCSTs. These tunable thermoresponsive properties were notably attributed to the architecture of the copolymers, determined by Jaacks method, which showed a slight difference of reactivity ratios of BCEEM and NiPAAm in the copolymer (respectively 1.29 and 0.86), preferentially generating a configuration with small blocks of both monomeric units. Determination of thermosensitive properties allowed the selection of P(BCEEM-*st*-NiPAAm) 13/87, which showed relatively high quantity of complexing moiety in combination with LCST value close to room temperature, thus enabling a low energetic cost when going from soluble to insoluble state while heating.

Sorption of lithium and competitive sorption in multicomponent solutions with P(BCEEM-*st*-NiPAAm) 13/87 were determined. For lithium, in optimal conditions, at 17 °C, pH = 10 after 24 h, the copolymer exhibited a Qmax of 0.075 mmol/g of polymer, which is in the lower range of reported sorption capacities for CE-based complexation. For competitive sorption, the polymer showed solution -dependant selectivity: in LIB leachate-like solutions, containing higher proportions of cobalt and lithium, the polymer was selective towards Li^+ and Co^{2+}, whereas in solutions with excess of bivalent ions, Ni^{2+} and Mn^{2+} were favoured. The rather low adsorption capacities compelled us to further investigate the thermodynamics and sorption mechanisms. DLS and UV-Vis measurements showed that the polymer presented salting-out effects when in the presence of lithium, forcing the polymer into a conformation that did not facilitate sorption processes. ITC experiments provided association constants values of respectively 11, 38, 41 and 63 M^{-1} for Li, Co, Ni and Mn. These values were in accordance with the literature for benzo-CEs, but relatively low compared to CEs without an aromatic, confirming that the globally low Qe observed along the study could be attributed to the rigid and hydrophobic benzo-group that is adjacent to the CE. The selectivity observed towards Li and Co in leachate-like solutions could be attributed to their simple excess compared to Ni and Mn, however increasing the proportion of all the metals towards the concentration of lithium caused a decrease in the adsorption capacity of lithium, since the polymer preferentially

interacted with the other ions individually. Adsorption performance of the material is relatively weak under studied conditions. As a consequence, sorption conditions remain to be optimized to envisage practical industrial applications. Improving the current adsorption capacity of the crown ethers while gaining selectivity towards lithium and maintaining adapted thermoresponsive properties is thus an ongoing challenge. In a forthcoming publication, long-term stability, and regeneration performances of the developed polymer materials will be reported, and we will also be keen to report synthesis and study of other functional materials in batch and dynamic processes, thus advancing lithium recovery technologies for battery applications.

6. References

[1] M. Wu, W. Chen, Forecast of Electric Vehicle Sales in the World and China Based on PCA-GRNN, Sustainability, 14 (2022) 2206.

[2] P. Xu, D.H.S. Tan, B. Jiao, H. Gao, X. Yu, Z. Chen, A Materials Perspective on Direct Recycling of Lithium-Ion Batteries: Principles, Challenges and Opportunities, Advanced Functional Materials, 33 (2023) 2213168.

[3] Roskill Information Services Ltd. Lithium : Outlook to 2028, in, 2019, pp. 501.

[4] Mineral commodity summaries 2021, in: Mineral Commodity Summaries, Reston, VA, 2021, pp. 200.

[5] European Parliament and Council of the European Union. Regulation (EU) 2020/740 of the European Parliament and of the Council of 25 May 2020 on batteries and waste batteries, amending Directive 2006/66/EC and repealing Regulation (EU) No 493/2012., in, Official Journal of the European Union., 2020, pp. 1-86.

[6] H. Bae, Y. Kim, Technologies of lithium recycling from waste lithium ion batteries: a review, Materials Advances, 2 (2021) 3234-3250.

[7] B. Makuza, Q. Tian, X. Guo, K. Chattopadhyay, D. Yu, Pyrometallurgical options for recycling spent lithium-ion batteries: A comprehensive review, Journal of Power Sources, 491 (2021) 229622.

[8] R. Sattar, S. Ilyas, H.N. Bhatti, A. Ghaffar, Resource recovery of critically-rare metals by hydrometallurgical recycling of spent lithium ion batteries, Separation and Purification Technology, 209 (2019) 725-733.

[9] V. Gunarathne, A.U. Rajapaksha, M. Vithanage, D.S. Alessi, R. Selvasembian, M. Naushad, S. You, P. Oleszczuk, Y.S. Ok, Hydrometallurgical processes for heavy metals recovery from industrial sludges, Critical Reviews in Environmental Science and Technology, 52 (2022) 1022-1062.

[10] L. Li, V.G. Deshmane, M.P. Paranthaman, R.R. Bhave, B.A. Moyer, S. Harrison, Lithium Recovery from Aqueous Resources and Batteries: A Brief Review, Johnson Matthey Technology Review, 62 (2018) Medium: ED; Size: p. 161-176.

[11] H. Yu, G. Naidu, C. Zhang, C. Wang, A. Razmjou, D.S. Han, T. He, H. Shon, Metal-based adsorbents for lithium recovery from aqueous resources, Desalination, 539 (2022) 115951.

[12] I. Oral, V. Abetz, A Highly Selective Polymer Material using Benzo-9-Crown-3 for the Extraction of Lithium in Presence of Other Interfering Alkali Metal Ions, Macromolecular Rapid Communications, 42 (2021) 2000746.

[13] M. Ali, I. Ahmed, P. Ramirez, S. Nasir, S. Mafe, C.M. Niemeyer, W. Ensinger, Lithium Ion Recognition with Nanofluidic Diodes through Host–Guest Complexation in Confined Geometries, Anal Chem, 90 (2018) 6820-6826.

[14] G.M. Nisola, K.J. Parohinog, R.E.C. Torrejos, S. Koo, S.-P. Lee, H. Kim, W.-J. Chung, Crown ethers "clicked" on fibrous polyglycidyl methacrylate for selective Li+ retrieval from aqueous sources, Colloids and Surfaces A: Physicochemical and Engineering Aspects, 596 (2020) 124709.

[15] H. Gohil, S. Chatterjee, S. Yadav, E. Suresh, A.R. Paital, An Ionophore for High Lithium Loading and Selective Capture from Brine, Inorganic Chemistry, 58 (2019) 7209-7219.

[16] J.M. Lehn, J.P. Sauvage, Cryptates. XVI. [2]-Cryptates. Stability and selectivity of alkali and alkaline-earth macrobicyclic complexes, Journal of the American Chemical Society, 97 (1975) 6700-6707.

[17] Z. Ren, X. Wei, R. Li, W. Wang, Y. Wang, Z. Zhou, Highly selective extraction of lithium ions from salt lake brines with sodium tetraphenylborate as co-extractant, Separation and Purification Technology, 269 (2021) 118756.

[18] J.W. Steed, First- and second-sphere coordination chemistry of alkali metal crown ether complexes, Coordination Chemistry Reviews, 215 (2001) 171-221.

[19] M.G. Hankins, T. Hayashita, S.P. Kasprzyk, R.A. Bartsch, Immobilization of Crown Ether Carboxylic Acids on Silica Gel and Their Use in Column Concentration of Alkali Metal Cations from Dilute Aqueous Solutions, Anal Chem, 68 (1996) 2811-2817.

[20] Z. Li, G. He, G. Zhao, J. Niu, L. Li, J. Bi, H. Mu, C. Zhu, Z. Chen, L. Zhang, H. Zhang, J. Zhang, B. Wang, Y. Wang, Preparation of a novel ion-imprinted membrane using sodium periodate-oxidized polydopamine as the interface adhesion layer for the direction separation of Li+ from spent lithium-ion battery leaching solution, Separation and Purification Technology, 277 (2021) 119519.

[21] Y. Sun, M. Zhu, Y. Yao, H. Wang, B. Tong, Z. Zhao, A novel approach for the selective extraction of Li+ from the leaching solution of spent lithium-ion batteries using benzo-15-crown-5 ether as extractant, Separation and Purification Technology, 237 (2020) 116325.

[22] K. Kobiro, New class of lithium ion selective crown ethers with bulky decalin subunits, Coordination Chemistry Reviews, 148 (1996) 135-149.

[23] R.E.C. Torrejos, G.M. Nisola, H.S. Song, L.A. Limjuco, C.P. Lawagon, K.J. Parohinog, S. Koo, J.W. Han, W.-J. Chung, Design of lithium selective crown ethers: Synthesis, extraction and theoretical binding studies, Chemical Engineering Journal, 326 (2017) 921-933.

[24] T. Hayashita, J.H. Lee, M.G. Hankins, J.C. Lee, J.S. Kim, J.M. Knobeloch, R.A. Bartsch, Selective sorption and column concentration of alkali-metal cations by carboxylic acid resins with dibenzo-14-crown-4 subunits and their acyclic polyether analogs, Anal Chem, 64 (1992) 815-819.

[25] B. Hashemi, M. Shamsipur, Z. Seyedzadeh, Synthesis of ion imprinted polymeric nanoparticles for selective pre-concentration and recognition of lithium ions, New Journal of Chemistry, 40 (2016) 4803-4809.

[26] X. Xu, F. Qiu, D. Yang, X. Zheng, Y. Wang, J. Pan, T. Zhang, J. Xu, C. Li, Dual-template crown ether-functionalized hierarchical porous silica: Preparation and application for adsorption of energy metal lithium, Applied Organometallic Chemistry, 32 (2018) e4114.

[27] W. Huang, S. Liu, J. Liu, W. Zhang, J. Pan, 2-Methylol-12-crown-4 ether immobilized PolyHIPEs toward recovery of lithium(i), New Journal of Chemistry, 42 (2018) 16814-16822.

[28] D. Sun, Y. Zhu, M. Meng, Y. Qiao, Y. Yan, C. Li, Fabrication of highly selective ion imprinted macroporous membranes with crown ether for targeted separation of lithium ion, Separation and Purification Technology, 175 (2017) 19-26.

[29] S.J. Warnock, R. Sujanani, E.S. Zofchak, S. Zhao, T.J. Dilenschneider, K.G. Hanson, S. Mukherjee, V. Ganesan, B.D. Freeman, M.M. Abu-Omar, C.M. Bates, Engineering Li/Na selectivity in 12-Crown-4–functionalized polymer membranes, Proceedings of the National Academy of Sciences, 118 (2021) e2022197118.

[30] L. Baudino, A. Pedico, S. Bianco, M. Periolatto, C.F. Pirri, A. Lamberti, Crown-Ether Functionalized Graphene Oxide Membrane for Lithium Recovery from Water, Membranes, 12 (2022) 233.

[31] X. Ji, C. Guo, W. Chen, L. Long, G. Zhang, N.M. Khashab, J.L. Sessler, Removal of Anions from Aqueous Media by Means of a Thermoresponsive Calix[4]pyrrole Amphiphilic Polymer, Chemistry – A European Journal, 24 (2018) 15791-15795.

[32] A. Graillot, S. Djenadi, C. Faur, D. Bouyer, S. Monge, J.J. Robin, Removal of metal ions from aqueous effluents involving new thermosensitive polymeric sorbent, Water Science and Technology, 67 (2013) 1181-1187.

[33] V. Aseyev, H. Tenhu, F.M. Winnik, Non-ionic Thermoresponsive Polymers in Water, in: A.H.E. Müller, O. Borisov (Eds.) Self Organized Nanostructures of Amphiphilic Block Copolymers II, Springer Berlin Heidelberg, Berlin, Heidelberg, 2011, pp. 29-89.

[34] A. Graillot, S. Monge, C. Faur, D. Bouyer, C. Duquesnoy, J.-J. Robin, How to easily adapt cloud points of statistical thermosensitive polyacrylamide-based copolymers knowing reactivity ratios, RSC Advances, 4 (2014) 19345-19355.

[35] J. Guan, Y. Li, Y. Guo, R. Su, G. Gao, H. Song, H. Yuan, B. Liang, Z. Guo, Mechanochemical Process Enhanced Cobalt and Lithium Recycling from Wasted Lithium-Ion Batteries, ACS Sustainable Chemistry & Engineering, 5 (2017) 1026-1032.

[36] C.K. Lee, K.-I. Rhee, Reductive leaching of cathodic active materials from lithium ion battery wastes, Hydrometallurgy, 68 (2003) 5-10.

[37] C.K. Lee, K.-I. Rhee, Preparation of LiCoO2 from spent lithium-ion batteries, Journal of Power Sources, 109 (2002) 17-21.

[38] S.P. Barik, G. Prabaharan, L. Kumar, Leaching and separation of Co and Mn from electrode materials of spent lithium-ion batteries using hydrochloric acid: Laboratory and pilot scale study, Journal of Cleaner Production, 147 (2017) 37-43.

[39] S. Dhiman, B. Gupta, Partition studies on cobalt and recycling of valuable metals from waste Li-ion batteries via solvent extraction and chemical precipitation, Journal of Cleaner Production, 225 (2019) 820-832.

[40] P. Meshram, B.D. Pandey, T.R. Mankhand, Hydrometallurgical processing of spent lithium ion batteries (LIBs) in the presence of a reducing agent with emphasis on kinetics of leaching, Chemical Engineering Journal, 281 (2015) 418-427.

[41] Q. Wei, Y. Wu, S. Li, R. Chen, J. Ding, C. Zhang, Spent lithium ion battery (LIB) recycle from electric vehicles: A mini-review, Science of The Total Environment, 866 (2023) 161380.

[42] M. Chen, X. Ma, B. Chen, R. Arsenault, P. Karlson, N. Simon, Y. Wang, Recycling End-of-Life Electric Vehicle Lithium-Ion Batteries, Joule, 3 (2019) 2622-2646.

[43] V. Jaacks, A novel method of determination of reactivity ratios in binary and ternary copolymerizations, Die Makromolekulare Chemie, 161 (1972) 161-172.

[44] S. Furyk, Y. Zhang, D. Ortiz-Acosta, P.S. Cremer, D.E. Bergbreiter, Effects of end group polarity and molecular weight on the lower critical solution temperature of poly(N-isopropylacrylamide), 44 (2006) 1492-1501.

[45] J. Lu, Y. Qin, Q. Zhang, Y. Wu, J. Cui, C. Li, L. Wang, Y. Yan, Multilayered ion-imprinted membranes with high selectivity towards Li+ based on the synergistic effect of 12-crown-4 and polyether sulfone, Applied Surface Science, 427 (2018) 931-941.

[46] R.E.C. Torrejos, G.M. Nisola, M.J. Park, H.K. Shon, J.G. Seo, S. Koo, W.-J. Chung, Synthesis and characterization of multi-walled carbon nanotubes-supported dibenzo-14-crown-4 ether with proton ionizable carboxyl sidearm as Li+ adsorbents, Chemical Engineering Journal, 264 (2015) 89-98.

[47] X.-J. Ju, L. Liu, R. Xie, C.H. Niu, L.-Y. Chu, Dual thermo-responsive and ion-recognizable monodisperse microspheres, Polymer, 50 (2009) 922-929.

[48] D. Huang, Q. Zhang, Y. Deng, Z. Luo, B. Li, X. Shen, Z. Qi, S. Dong, Y. Ge, W. Chen, Polymeric crown ethers: LCST behavior in water and stimuli-responsiveness, Polymer Chemistry, 9 (2018) 2574-2579.

[49] T. Matsuoka, S.-i. Yamamoto, O. Moriya, M. Kashio, T. Sugizaki, Synthesis of thermoresponsive polysilsesquioxane with methoxyethylamide group and crown ether, Polymer Journal, 42 (2010) 313-318.

[50] H.-R. Yu, J.-Q. Hu, X.-H. Lu, X.-J. Ju, Z. Liu, R. Xie, W. Wang, L.-Y. Chu, Insights into the Effects of 2:1 "Sandwich-Type" Crown-Ether/Metal-Ion Complexes in Responsive Host–Guest Systems, The Journal of Physical Chemistry B, 119 (2015) 1696-1705.

[51] D. Gomes Rodrigues, N. Dacheux, S. Pellet-Rostaing, C. Faur, D. Bouyer, S. Monge, The first report on phosphonate-based homopolymers combining both chelating and thermosensitive properties of gadolinium: synthesis and evaluation, Polymer Chemistry, 6 (2015) 5264-5272.

[52] J. Cui, Z. Zhou, S. Liu, Y. Zhang, L. Yan, Q. Zhang, S. Zhou, Y. Yan, C. Li, Synthesis of cauliflower-like ion imprinted polymers for selective adsorption and separation of lithium ion, New Journal of Chemistry, 42 (2018) 14502-14509.

[53] J. Cui, Y. Zhang, Y. Wang, J. Ding, P. Yu, Y. Yan, C. Li, Z. Zhou, Fabrication of lithium ion imprinted hybrid membranes with antifouling performance for selective recovery of lithium, New Journal of Chemistry, 42 (2018) 118-128.

[54] X. Luo, B. Guo, J. Luo, F. Deng, S. Zhang, S. Luo, J. Crittenden, Recovery of Lithium from Wastewater Using Development of Li Ion-Imprinted Polymers, ACS Sustainable Chemistry & Engineering, 3 (2015) 460-467.

[55] C. Yuan, L. Zhang, H. Li, R. Guo, M. Zhao, L. Yang, Highly Selective Lithium Ion Adsorbents: Polymeric Porous Microsphere with Crown Ether Groups, Transactions of Tianjin University, 25 (2019) 101-109.

[56] L.A. Limjuco, G.M. Nisola, R.E.C. Torrejos, J.W. Han, H.S. Song, K.J. Parohinog, S. Koo, S.-P. Lee, W.-J. Chung, Aerosol Cross-Linked Crown Ether Diols Melded with Poly(vinyl alcohol) as Specialized Microfibrous Li+ Adsorbents, ACS Applied Materials & Interfaces, 9 (2017) 42862-42874.

[57] Y. Marcus, A simple empirical model describing the thermodynamics of hydration of ions of widely varying charges, sizes, and shapes, Biophysical Chemistry, 51 (1994) 111-127.

[58] Y. Luo, N. Marets, T. Kato, Selective lithium ion recognition in self-assembled columnar liquid crystals based on a lithium receptor, Chemical Science, 9 (2018) 608-616.

[59] S.S. Dixit, M.S. Shashidhar, Inositol derived crown ethers: effect of auxiliary protecting groups and the relative orientation of crown ether oxygen atoms on their metal ion binding ability, Tetrahedron, 64 (2008) 2160-2171.